

# An imperfect double: probing the physical origin of the low-frequency QPO and its harmonic in black hole binaries

Magnus Axelsson,<sup>1,2\*</sup> Chris Done<sup>3</sup> and Linnea Hjalmsdotter<sup>4</sup>

<sup>1</sup>*Oskar Klein Center for CosmoParticle Physics, Department of Physics, Stockholm University, SE-106 91 Stockholm, Sweden*

<sup>2</sup>*Department of Astronomy, Stockholm University, SE-106 91 Stockholm, Sweden*

<sup>3</sup>*Department of Physics, Durham University, South Road, Durham DH1 3LE, UK*

<sup>4</sup>*Sternberg Astronomical Institute, Moscow State University, Universitetskij pr. 13, 119899 Moscow, Russia*

Accepted –. Received –; in original form –

## ABSTRACT

We extract the spectra of the strong low-frequency quasi-periodic oscillation (QPO) and its harmonic during the rising phase of an outburst in the black-hole binary XTE J1550-564. We compare these frequency resolved spectra to the time-averaged spectrum and the spectrum of the rapid ( $< 0.1$ s) variability. The spectrum of the time averaged emission can be described by a disc, a Compton upscattered tail, and its reflection. The QPO spectrum is very similar to the spectrum of the most rapid variability, implying it arises in the innermost regions of the flow. It contains little detectable disc, and its Compton spectrum is generally harder and shows less reflection than in the time averaged emission. The harmonic likewise contains little detectable disc component, but has a Compton spectrum which is systematically softer than the QPO, softer even than the Compton tail in the time averaged emission. We interpret these results in the context of the truncated disc model, where the inner disc is replaced by a hot flow. The QPO can arise in this picture from vertical (Lense-Thirring) precession of the entire hot inner flow, and its harmonic can be produced by the angular dependence of Compton scattering within the hot flow. We extend these models to include stratification of the hot flow, so that it is softer (lower optical depth) at larger radii closer to the truncated disc, and harder (higher optical depth) in the innermost parts of the flow where the rapid variability is produced. The different optical depth with radius gives rise to different angular dependence of the Comptonised emission, weighting the fundamental to the inner parts of the hot flow, and the harmonic to the outer. This is the first model which can explain both the spectrum of the QPO, and its harmonic, in a self consistent geometry.

**Key words:** Accretion, accretion discs – X-rays: binaries – X-rays: individual (XTE J1550-564)

## 1 INTRODUCTION

The correlated spectral and variability properties seen in accreting black hole systems can be explained if the inner disc truncates at some radius above the last stable orbit, evaporating into a hot inner flow. Hot electrons in the inner flow up-scatter the soft disc photons, giving rise to a Comptonised component in the spectrum. Decreasing the transition radius as the mass accretion rate increases from the low/hard to high/soft state gives both a qualitative and quantitative description of the spectral softening (both

increase in disc component and increasing softness of the Comptonised tail due to the larger cooling flux of seed photons from the disc) and decrease in low frequency components of the power spectral density (e.g., Done, Gierliński & Kubota 2007).

The lack of an inner disc means the flow can vertically precess due to misalignment between the black hole spin and accretion flow (Lense-Thirring precession). This is strongly differential for single particle orbits, but for a viscously connected hot flow it can result in global precession of the entire flow (Lubow et al. 2002). This global precession is seen in numerical simulations (Fragile et al. 2007), and is a strong candidate to explain the origin of the strong low-frequency

\* email: magnusa@astro.su.se

quasi-periodic oscillation (QPO) seen in many black hole binaries (Fragile et al. 2007; Ingram et al. 2009). Ingram et al. (2009) show that this scenario naturally explains the fact that the energy spectrum of the QPO is dominated by the Comptonised emission rather than the blackbody disk (see, e.g., Remillard & McClintock 2006).

However, the structure of the hot flow is probably not simply a single temperature, single optical depth Comptonising region. Cygnus X-1 shows clear evidence for two different regions in its Comptonised spectrum close to the hard/soft spectral transition (Yamada et al. 2013). Spectral inhomogeneity is clearly required in order to explain the complex pattern of time lags in the data (Miyamoto & Kitamoto 1989), where slow variability stirred up at large radii (softer spectra) in the hot flow propagates down to smaller radii, giving a lagged modulation of a harder spectrum (Kotov et al. 2001; Arévalo & Uttley 2006). This correlation of spectral shape with timescale is seen directly in Cyg X-1 using frequency resolved spectra (Revnivtsev et al. 1999). This has an immediate interpretation in the context of the truncated disc/hot inner flow model as the outer parts of the hot flow are closer to the disc, so intercept more seed photons so the spectrum should be softer than in the inner regions of the flow which are more seed photon starved.

In Axelsson et al. (2013, hereafter Paper I) we used frequency resolved spectroscopy to study the spectrum of the fastest variability through a hard/soft transition. We found that it contained no contribution from the disk blackbody, significantly less reflection and a harder Comptonised spectrum than the time averaged continuum, in agreement with the picture above of the innermost region of the hot flow. Here we extend the frequency resolved spectral study to the QPO and its harmonic in XTE J1550-564.

Previous studies of the QPO spectrum have shown that both the rapid variability and QPOs are tied predominantly to the Comptonised emission rather than the disk (e.g., Churazov et al. 2001; Gilfanov et al. 2003). However, Sobolewska & Życki (2006) did more detailed modelling of the QPO spectrum, and were able to fit many of these using purely ionized reflection rather than the direct Comptonised emission. Here we use the improved models of ionized reflection developed in Paper I to reassess the contribution of reflection to the QPO spectrum, especially as these models show that the very similar spectrum of the fastest variability contains very little reflection (Paper I). We find that the QPO spectra are better fit by Comptonisation models, with little reflection, similar to the fastest variability spectra in Paper I and consistent with being produced in the same innermost regions of the hot flow.

The harmonic of the QPO is strong in the observations of XTE J1550-564 considered here, with rms ranging from 0.3-0.5 times that of the fundamental (Cui et al. 1999). Such a feature has also been seen in other black hole transient systems, for example GX 339-4 (Belloni et al. 2005). There are no previous studies of the detailed spectrum of the harmonic, though it is clear that it is systematically softer than the QPO (Cui et al. 1999). Recent work by Veledina et al. (2013b) has shown that the existence of a strong harmonic is predicted by the angular radiation pattern from Comptonisation of a precessing hot inner flow. We use this model to interpret the harmonic spectra, and find that this is also consistent with the inhomogeneous hot flow model discussed

above, as the harmonic should be stronger in the spectra from regions of lower optical depth, weighting the harmonic to the outer (softer) regions of the hot flow. This is the first model to explain both the QPO and its harmonic in the same inhomogeneous hot flow geometry as required to explain the time lags.

## 2 DATA ANALYSIS

In this study we use archival data of XTE J1550-564 from the Proportional Counter Array (PCA; Jahoda et al. 1996) instrument onboard the *RXTE* satellite. The observations are made in the time period 1998-09-09 to 1998-09-16 (MJD 51065 to 51072) and cover the rise of the strong initial flare of the 1998 outburst (for more details on this outburst see Smith 1998).

To extract the spectra of the QPO and harmonic, we follow the same procedure as in Paper I. In every observation we extracted a light curve for each available channel and constructed a power density spectrum. To determine the contribution of the QPO/harmonic we fit these features using Lorentzian functions, which were then integrated to produce the rms variability. Finally, combining the results for all channels allows us to build the energy spectrum of the QPO/harmonic.

As in Paper I, we follow the standard approach and add a systematic error of 1 per cent to all bins. We note that this leads to the systematics dominating the uncertainties for the average spectra, as seen by the extremely low values of  $\chi^2/\text{dof}$ . In Paper I, the additional errors introduced via the power spectrum meant that systematics did not dominate the rms spectra of the fastest ( $> 10$  Hz) variability. However, the QPO has more variability power, so the QPO spectra are better determined so systematics can dominate the QPO spectra.

The data were fit in XSPEC using the same spectral model as in Paper I: a disc blackbody (DISKBB; Mitsuda et al. 1984), thermal Comptonization (NTHCOMP; Życki, Done & Smith 1999) with seed photons tied to the inner disc temperature, and reflection of the Compton spectrum (RFXCONV, based on the Ross & Fabian 2005 ionised reflection tables, but re-coded into a convolution form so they can be used on any continuum; Kohlemainen, Done & Díaz Trigo 2011). We note that this reflection model is more physical than the PEXRIV based ionised reflection models used by Sobolewska & Życki (2006) as it includes Comptonisation within the disc photosphere itself which broadens the line and edge features (Young et al. 2001). We fix the inclination at  $70^\circ$ , as determined from the orbital elements of the system (Orosz et al. 2002). We also include an absorption line (GABS), in order to model absorption through a wind from the disc as is generally seen in high inclination systems (Ponti et al. 2012).

## 3 RESULTS

Table 1 shows the results of fitting our spectral model to the data. For comparison, we also include the fits of the rapid variability and continuum spectrum from Paper I. The model above gives an adequate fit  $\chi^2/\text{dof} \sim 1$  to both the QPO and harmonic data.

ObsID	$T_{\text{bb}}$ (keV)	$N_{\text{bb}}$	$\Gamma$	$kT_e$ (keV)	$R$	$E_{\text{line}}$ (keV)	EW ( $\times 10^{-2}$ keV)	$\log \xi$	$\chi^2/dof$	Flux $\text{erg cm}^{-2} \text{s}^{-1}$
30188-06-01-00	$0.56^{+0.31}_{-0.26}$	$200^{+570}_{-200}$	$1.77^{+0.03}_{-0.10}$	$14.8^{+7.3}_{-3.0}$	$0.44^{+0.12}_{-0.11}$	$6.84^{+0.11}_{-0.11}$	$9.5^{+4.0}_{-2.7}$	$2.80^{+0.03}_{-0.09}$	2.3/36	$4.4 \times 10^{-8}$
rms			$1.69^{+0.03}_{-0.03}$		$0.07^{+0.09}_{-0.07}$				17.4/54	
qpo		$0^{+360}_{-0}$	$1.72^{+0.02}_{-0.02}$		$0.06^{+0.12}_{-0.06}$				5.9/54	
harmonic		$0^{+200}_{-0}$	$1.92^{+0.05}_{-0.06}$		$0.50^{+0.28}_{-0.23}$				5.8/49	
30188-06-01-01	$0.55^{+0.04}_{-0.04}$	$260^{+590}_{-260}$	$1.80^{+0.03}_{-0.04}$	$15.1^{+5.8}_{-3.0}$	$0.43^{+0.14}_{-0.11}$	$6.85^{+0.09}_{-0.09}$	$9.2^{+3.5}_{-3.6}$	$2.80^{+0.67}_{-0.09}$	7.0/36	$4.0 \times 10^{-8}$
rms			$1.66^{+0.09}_{-0.08}$		$0.06^{+0.25}_{-0.06}$				50.8/54	
qpo		$220^{+660}_{-220}$	$1.80^{+0.03}_{-0.03}$		$0.23^{+0.18}_{-0.16}$				23.4/54	
harmonic		$0^{+230}_{-0}$	$1.95^{+0.03}_{-0.05}$		$0.01^{+0.10}_{-0.01}$				24.0/49	
30188-06-01-02	$0.55^{+0.28}_{-0.08}$	$410^{+1100}_{-410}$	$1.89^{+0.02}_{-0.02}$	$10.6^{+2.4}_{-1.5}$	$0.56^{+0.15}_{-0.14}$	$6.83^{+0.10}_{-0.09}$	$11^{+5.0}_{-4.7}$	$2.78^{+0.60}_{-0.09}$	4.5/36	$4.3 \times 10^{-8}$
rms			$1.78^{+0.03}_{-0.03}$		$0.0^{+0.07}_{-0.0}$				35.2/54	
qpo		$0^{+63}_{-0}$	$1.79^{+0.01}_{-0.01}$		$0.22^{+0.07}_{-0.07}$				55.4/54	
harmonic		$0^{+67}_{-0}$	$2.07^{+0.03}_{-0.03}$		$0.27^{+0.12}_{-0.11}$				43.9/47	
30188-06-01-03	$0.53^{+0.25}_{-0.09}$	$970^{+1100}_{-970}$	$1.94^{+0.03}_{-0.09}$	$10.9^{+2.3}_{-1.6}$	$0.52^{+0.15}_{-0.16}$	$6.80^{+0.08}_{-0.08}$	$9.6^{+2.5}_{-3.7}$	$2.78^{+0.70}_{-0.08}$	7.0/36	$4.4 \times 10^{-8}$
rms			$1.79^{+0.03}_{-0.05}$		$0.07^{+0.21}_{-0.07}$				17.8/54	
qpo		$0^{+250}_{-0}$	$1.76^{+0.03}_{-0.03}$		$0.33^{+0.17}_{-0.14}$				41.2/54	
harmonic		$0^{+182}_{-0}$	$2.03^{+0.04}_{-0.04}$		$0.13^{+0.14}_{-0.13}$				23.1/47	
30188-06-04-00	$0.53^{+0.19}_{-0.53}$	$4100^{+1200}_{-2000}$	$2.03^{+0.03}_{-0.03}$	$9.9^{+1.7}_{-0.7}$	$0.54^{+0.17}_{-0.15}$	$6.82^{+0.09}_{-0.09}$	$9.6^{+2.9}_{-3.9}$	$2.79^{+0.68}_{-0.05}$	6.1/36	$5.1 \times 10^{-8}$
rms			$1.90^{+0.03}_{-0.03}$		$0.33^{+0.12}_{-0.11}$				38.9/54	
qpo		$0^{+90}_{-0}$	$1.87^{+0.01}_{-0.01}$		$0.43^{+0.10}_{-0.10}$				48.7/54	
harmonic		$0^{+86}_{-0}$	$2.25^{+0.03}_{-0.03}$		$0.42^{+0.13}_{-0.12}$				40.7/47	
30188-06-05-00	$0.58^{+0.08}_{-0.58}$	$8400^{+880}_{-2800}$	$2.19^{+0.07}_{-0.04}$	$11.6^{+3.3}_{-1.4}$	$0.54^{+0.20}_{-0.17}$	$6.81^{+0.10}_{-0.11}$	$9.0^{+3.9}_{-2.9}$	$2.81^{+0.18}_{-0.22}$	6.0/36	$6.0 \times 10^{-8}$
rms			$2.01^{+0.03}_{-0.03}$		$0.10^{+0.10}_{-0.10}$				28.2/54	
qpo		$0^{+51}_{-0}$	$2.03^{+0.01}_{-0.01}$		$0.48^{+0.12}_{-0.11}$				84.2/54	
harmonic		$400^{+450}_{-370}$	$2.33^{+0.06}_{-0.06}$		$0.10^{+0.23}_{-0.10}$				39.9/47	
30188-06-06-00	$0.65^{+0.08}_{-0.45}$	$9100^{+540}_{-1000}$	$2.33^{+0.06}_{-0.06}$	$11.5^{+4.5}_{-1.5}$	$0.70^{+0.19}_{-0.20}$	$6.80^{+0.08}_{-0.09}$	$11^{+2.7}_{-3.7}$	$2.75^{+0.17}_{-0.16}$	5.6/36	$5.4 \times 10^{-8}$
rms			$2.07^{+0.02}_{-0.04}$		$0.30^{+0.25}_{-0.13}$				38.7/54	
qpo		$0^{+22}_{-0}$	$2.14^{+0.01}_{-0.01}$		$0.54^{+0.06}_{-0.10}$				111/54	
harmonic		$340^{+230}_{-190}$	$2.51^{+0.08}_{-0.08}$		$0.59^{+0.21}_{-0.19}$				6.4/47	
30188-06-07-00	$0.70^{+0.07}_{-0.51}$	$6600^{+350}_{-560}$	$2.27^{+0.08}_{-0.06}$	$10.4^{+2.7}_{-1.0}$	$0.64^{+0.15}_{-0.20}$	$6.81^{+0.08}_{-0.08}$	$11^{+3.0}_{-3.4}$	$2.78^{+0.23}_{-0.22}$	6.3/36	$6.4 \times 10^{-8}$
rms			$2.11^{+0.03}_{-0.03}$		$0.29^{+0.08}_{-0.11}$				35.8/54	
qpo		$0^{+38}_{-0}$	$2.12^{+0.01}_{-0.01}$		$0.46^{+0.10}_{-0.09}$				36/54	
harmonic		$0^{+24}_{-0}$	$2.35^{+0.03}_{-0.03}$		$0.49^{+0.10}_{-0.10}$				16/47	
30188-06-09-00	$0.66^{+0.08}_{-0.45}$	$9600^{+480}_{-900}$	$2.39^{+0.08}_{-0.05}$	$12.8^{+5.3}_{-1.9}$	$0.67^{+0.16}_{-0.20}$	$6.79^{+0.08}_{-0.08}$	$9.5^{+3.0}_{-3.1}$	$2.73^{+0.14}_{-0.16}$	6.4/36	$6.7 \times 10^{-8}$
rms			$2.08^{+0.03}_{-0.03}$		$0.22^{+0.13}_{-0.12}$				21.8/54	
qpo		$0^{+78}_{-0}$	$2.24^{+0.01}_{-0.01}$		$0.31^{+0.09}_{-0.09}$				69.5/54	
harmonic		$0^{+37}_{-0}$	$2.48^{+0.03}_{-0.03}$		$0.50^{+0.13}_{-0.12}$				25.8/47	

**Table 1.** Fit results for the model TBABS×GABS×(DISKBB+NTHCOMP+NTHCOMP×RFXCONV). Errors indicate 90% confidence intervals.

### 3.1 Spectrum of QPO and rapid variability

The full details of the fits to all spectra through the transition are given in Table 1, while Fig. 1 shows the time averaged (total) continuum and spectrum of the QPO at the start, midpoint and end of the hard/soft transition. The time averaged Compton spectrum (black points in the top panel) softens dramatically as the source makes the transition, with an increasing amount of disc and disc reflection present. The QPO spectrum (red points in the top panel) is fit with the same model components, but with the spectral index of the

Comptonised emission, and the amount of disc and reflection allowed to vary. The next lowest panel for each ObsID shows the QPO spectral model residuals (red points).

Below the fit results, we also present three panels where we compare the best-fit results of the QPO to other components. The first panel shows the ratio of QPO spectrum to the model fit to the rapid variability ( $> 10$  Hz: blue points from Paper I). The QPO spectrum is always similar to that of the rapid variability throughout the outburst. Thus we expect (and see) similar parameters in the fits in Table 1 as for the spectrum of the rapid variability in Paper I. This

shows that the QPO spectrum is well described by thermal Comptonisation with only a small amount of reflection, in contrast to the reflection dominated fits of Sobolewska & Życki (2006), due to our use of more sophisticated reflection models (see Paper I). The lack of a strong disc component in the QPO spectrum can clearly be seen in the next panel down, which shows the ratio of the QPO spectrum to the model fit to the time averaged data (total spectrum: green points). There is a clear drop in this ratio at low energies where the disc component contributes.

The fact that there is less disc and less reflection in the QPO spectrum means that to zeroth order it is well described by the thermal Compton emission alone. However, more subtle effects can be seen in the bottom panel, which shows the ratio of the QPO spectrum to the model of thermal Comptonisation fit to the time averaged spectrum (orange points). The QPO spectrum evolves from being consistent with the Comptonised emission of the time averaged spectrum in the hardest states, to being increasingly harder than the time averaged spectrum as the source makes the transition, which is indeed the same behaviour as was seen in the rapid variability spectrum of Paper I, making it very likely that the QPO and rapid variability arise in the same region of the accretion flow.

### 3.2 The spectrum of the harmonic

Figure 2 shows the same spectra as in Fig. 1, with the vertical panels showing the same sequence of comparisons except for this figure we select the harmonic of the QPO rather than the fundamental. In agreement with the results found by Cui et al. (1999), we find that the harmonic becomes very weak at higher energies, and we are unable to constrain it in the power spectrum above  $\sim 12$  Hz. Interestingly, in the hardest observations it is seen up to somewhat higher energies (first two spectra in Fig. 2).

The harmonic is well fit by the same model components (red points, top and second panel), but with very different parameters (Table 1). The harmonic is noticeably steeper than the rapid variability (blue points), and is not so different to the total spectrum (green points), although there is still a drop at energies corresponding to the disc emission, again signalling that the direct disc emission is not being modulated (see also Table 1). Instead, the ratio of the harmonic to the Compton spectrum alone (orange, bottom panel) shows that the harmonic is systematically softer than the Comptonised component of the time averaged spectrum. More subtly, Table 1 also hints that there could be more reflection in the harmonic than in the QPO.

Thus it is clear that the harmonic arises in a different environment than the QPO. The fact that the harmonic spectrum is softer than the QPO and shows stronger signs of reflection points to the harmonic arising further out in the flow, in a region seeing more soft seed photons and where the disc subtends a larger solid angle.

### 3.3 Limitations of the spectral fits

While the fit statistics show that the fits are generally good, the residuals of the fits in the softer states hint that there may still be details not fully captured by our model. We tied

the Comptonisation seed photon temperature to be the same as that of the observed disc component seen in the average spectrum, yet the suggested geometry for the softer states has the inner disc extending underneath the outer parts of the corona. The corona is translucent, with optical depth  $\sim 1 - 2$  so photons from the disc underneath the corona are not observed as they are all Compton scattered. Thus these form the predominant source of seed photons, and are higher temperature than the observed disc emission which comes from further out in the disc (see Done & Kubota 2006 for a detailed discussion of this). We can find better fits by allowing the seed photon temperature in the corona to be higher than that of the observed disc emission. However, this seed photon temperature cannot be easily constrained from the time average spectrum alone as the observed disc overlaps the energy band of the downturn. The lack of a strong disc component in the QPO spectra means that these are more sensitive to the seed photon energy of the Comptonised emission than the corresponding time average spectra. However, the QPO spectra are of limited quality - there are only 13 data points in each spectrum - and hence they cannot reasonably constrain the seed photon temperature as well as the amount of reflection, Compton spectral index and normalisation of the disc and Compton components.

We explore possible consequences of this limitation by stepwise increasing the seed photon temperature for the time averaged and QPO spectra (always using the same value for both datasets). We find that this indeed allows us to find fits where the residuals seen in Fig. 1 mostly disappear. The resulting parameters show very similar trends to those presented above, in that the Compton spectrum of the QPO is generally harder, and has less reflection than that of the time average spectrum.

## 4 DISCUSSION

Although there have been many proposed mechanisms for QPOs in black-hole binaries, these have focussed mainly on how to match the observed characteristic frequencies rather than the spectrum of the QPO. Ingram et al. (2009) showed that vertical precession of the entire hot inner flow, as seen in the numerical simulations of Fragile et al. (2007), could provide a mechanism for both the frequency and spectrum of the QPO. Precession of the hot flow imprints the modulation onto the spectrum of the hot flow, naturally explaining the similarity between the QPO spectrum and the Comptonised emission in the continuum spectrum, and the lack of disc in the QPO.

This model can also be extended to encompass the broadband variability as well as the QPO (Ingram & Done 2011, 2012), by propagating fluctuations down through the entire precessing hot flow. This gives a framework in which to interpret the more subtle features seen in the QPO spectrum, and in the spectra of the most rapid variability (Paper I). The most rapid variability is only produced in the very inner region of the flow, while slower variability is produced at larger radii, and propagates down to the inner regions. All the hot flow within the truncated disc can precess vertically, but the regions furthest from the disc (i.e., closer to the centre) have harder spectra and produce less reflection as they subtend a smaller solid angle to the disc and

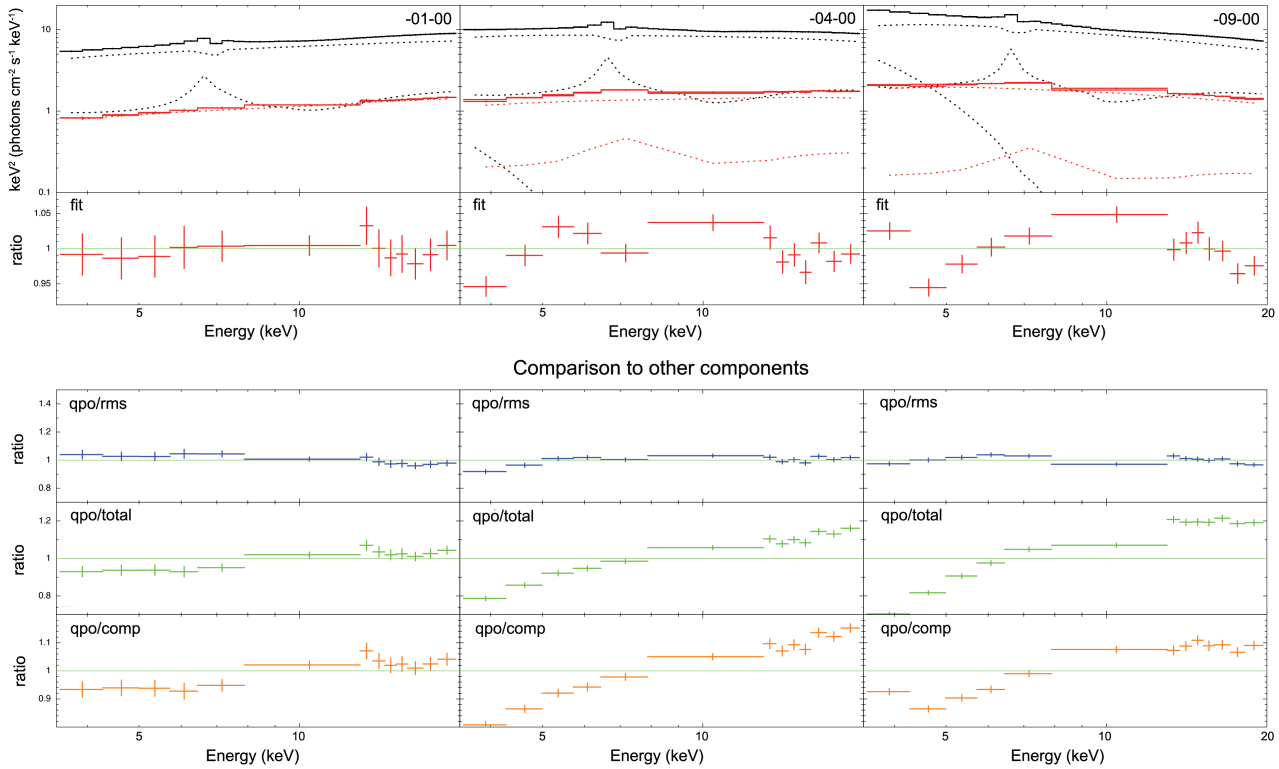


**Figure 1.** Top panel shows fits to the time averaged spectrum (black) and QPO (red). The second panel shows the ratio of the QPO spectrum (red) to the model fit in the upper panel, showing that the model describes the data well. Further down, the third panel shows the ratio between the QPO spectrum and the best-fit model for the rapid variability (blue), showing their similarity. The fourth panel shows the ratio of the QPO spectrum (green) to the time averaged continuum. There is a clear drop at low energies when the disc dominates, showing that the QPO does not modulate the disc emission. The bottom panel shows the ratio when comparing the QPO spectrum to only the Comptonised component from the time averaged continuum (orange). The QPO is subtly harder than the time averaged Comptonised emission, by an increasing amount as the spectrum softens.

are shielded from the disc by the radial optical depth of the rest of the flow. In the softest spectra seen here, the disc probably extends underneath the outer parts of the corona, preventing these regions from vertically precessing. Only the very innermost parts of the flow can precess, and these have the fastest stochastic variability and the hardest spectra.

This picture then explains the similarity of the QPO and rapid variability. However, it can also explain the difference in spectrum of the QPO and its harmonic. The harmonic is clearly softer than the QPO, but again this is mostly a change in the Compton continuum shape rather than in the amount of disc emission as the harmonic contains little detectable disc component.

Instead, in the context of a Compton scattering slab viewed at an angle  $\theta$ , the observed flux can be well approximated by (Pozdnyakov, Sobol & Sunyaev 1983; Viironen & Poutanen 2004)

$$F_E(\theta) \propto I(\theta) \cos \theta \approx (1 + b \cos \theta) \cos \theta = b/2 + \cos \theta + b/2 \cos 2\theta. \quad (1)$$

This approximation is fairly good even when  $I(\theta)$  is not well described by  $(1 + b \cos \theta)$  (J. Poutanen, priv. comm., see also Pozdnyakov, Sobol & Sunyaev 1983; Poutanen & Gierliński 2003). This means that the relative strength of the harmonic to QPO is set by  $|b|$ , which is dependent on the optical depth (Pozdnyakov, Sobol & Sunyaev 1983; Poutanen & Gierliński 2003). Lower optical depths give rise to larger  $|b|$ , so produce

stronger harmonics (see, e.g., fig. 2 in Viironen & Poutanen 2004).

The optical depth and/or temperature must increase with radius in the inhomogeneous picture for the Comptonised region developed to explain the spectral lags, so that harder spectra come from the innermost regions (Kotov et al. 2001; Arévalo & Uttley 2006). Our spectral fits assumed that the electron temperature remains constant throughout the region (i.e., that only the optical depth changes to make the change in spectral index). Thus in our fits the optical depth for the outer regions must be lower than in the harder, innermost regions, and thus the softer outer regions of the flow will contribute more to the harmonic spectrum. This means that the harmonic has a stronger contribution from the parts of the flow closest to the disc, matching the observational results of a softer spectrum and higher reflection.

A more quantitative result would require constraining the electron temperature in the inner and outer regions independently of the optical depth, which is beyond the current data. It should also depend on the scale height and/or detailed shape of the precessing flow. Equation 1 is strictly valid only for a slab, whereas we expect that the hot flow has an appreciable scale height and shape which also has a role in modulating the emission (Ingram & Done 2012). It also assumes that relativistic effects are negligible (i.e., typical radii are some  $\sim$  tens of Schwarzschild radii). Closer to

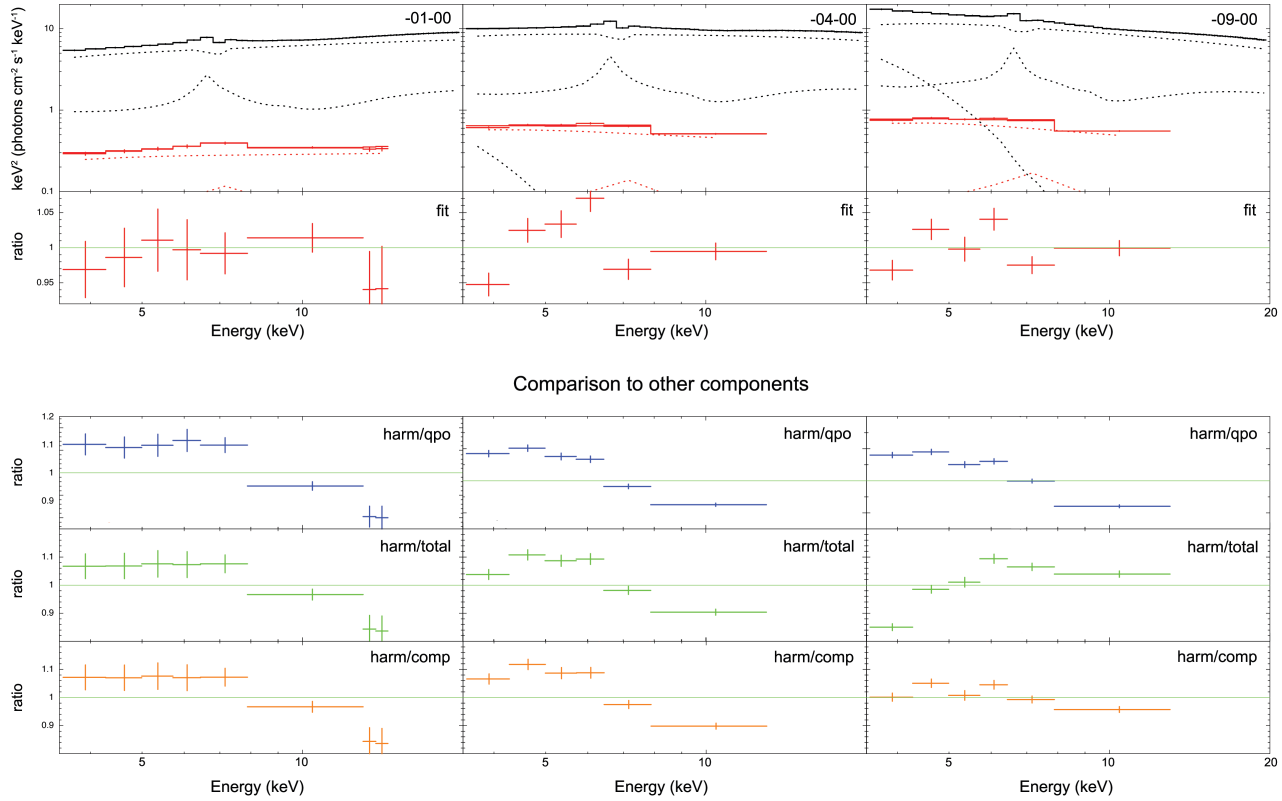


**Figure 2.** Fit of continuum spectrum and harmonic (top panel for each fit) along with residuals of the fit (red). Lower panels in each spectrum show the ratio between the harmonic data and best-fit models for the QPO (blue) and continuum (green). The harmonic is noticeably softer than the QPO and is not so different from the total spectrum, although there is still a drop at energies corresponding to the disc emission, signalling that the direct disc emission is not being modulated. The bottom panel shows the ratio when comparing the spectrum of the harmonic to only the Comptonised component from the continuum (orange).

the black hole, effects such as stronger gravitational curvature and faster Keplerian motion cause the dependence of the flux on  $\cos \theta$  to be weaker (Poutanen & Gierliński 2003). Together these effects could make substantial differences to the very simple model above, but the principle of a stronger contribution to the harmonic in the outer regions should remain.

Finally, we note that the Comptonised emission is expected to be polarized (Pozdnyakov, Sobol & Sunyaev 1983; Viironen & Poutanen 2004), and a precessing flow would mean that a QPO will be present in the polarization signal as well. Such a detection would therefore give extremely strong support to the Lense-Thirring origin of the QPO.

## 5 SUMMARY AND CONCLUSIONS

We have presented the first systematic analysis of the QPO spectrum through a hard/soft transition. We confirm previous results that it contains little detectable disc component, and for the first time show that its Compton spectrum is generally harder than in the time averaged emission, with less reflection. This makes it very similar to the spectrum of the rapid ( $> 10$  Hz) variability. Additionally, for the first time, we show the detailed spectrum of the harmonic. Like the QPO, this shows little detectable disc component,

but unlike the QPO it shows Comptonised emission which is softer than the Comptonisation component in the time-averaged continuum. The results are matched by expectations from the recently proposed scenario where the QPO is caused by Lense-Thirring precession of the entire hot inner flow. This model *predicts* the existence of harmonic structure to the QPO due to the angular distribution of the Comptonised emission coupled to the precession. The difference in spectra between the QPO and its harmonic can be additionally explained if the flow is radially stratified, with optical depth increasing towards the inner regions of the flow as this weights the harmonic towards the outer regions of the flow, where the spectrum is softer and produces more reflection. This framework is thus the first physical model encompassing both the QPO and harmonic.

## ACKNOWLEDGMENTS

This work was supported by The Royal Swedish Academy of Sciences and has made use of data obtained through the High Energy Astrophysics Science Archive Research Center (HEASARC) Online Service, provided by NASA/Goddard Space Flight Center. We thank Adam Ingram and Juri Poutanen for helpful discussions.

## REFERENCES

- Arévalo P., & Uttley P., 2006, MNRAS, 367, 801
- Axelsson M., Hjalmarsdotter L. Done, C., 2013, MNRAS, 431, 1987
- Belloni T., Homan J., Casella P. et al., 2005, A&A, 440, 207
- Churazov E., Gilfanov M., Revnivtsev M., 2001, MNRAS, 321, 759
- Cui W., Zhang S., Chen W., Morgan. E., 1999, ApJ, 512, L43
- Done C., & Kubota A., 2006, MNRAS, 371, 1216
- Done C., Gierliński M., Kubota A., 2007, A&ARv, 15, 1
- Fragile C. P., Blaes O. M., Anninos P., Salomonson J. D., 2007, ApJ, 668, 417
- Gilfanov M., Revnivtsev M., Molkov S., 2003, A&A, 410, 217
- Ingram A., Done C., Fragile P. C., 2009, MNRAS, 397, L101
- Ingram A. & Done C., 2011, MNRAS, 415, 2323
- Ingram A. & Done C., 2012, MNRAS, 419, 2369
- Jahoda K., Swank J. H., Giles A. B. et al., 1996, Proc. SPIE, 2808, 59
- Kohlemainen M., Done C., Diaz Trigo M., 2011, MNRAS, 416, 311
- Kotov O., Churazov E., Gilfanov M., 2001, MNRAS, 327, 799
- Lubow S. H., Ogilvie G. I., & Pringle J. E., 2002, MNRAS, 337, 706
- Mitsuda K., Inoue H., Koyama K. et al., 1984, PASJ, 36, 741
- Miyamoto S., & Kitamoto S., 1989, Nature, 342, 773
- Orosz J. A., Groot P. J., van der Klis M. et al., 2002, ApJ, 568, 845
- Ponti G., Fender R. P., Begelman M. C. et al. 2012, MNRAS, 422, L11
- Pozdnyakov L. A., Sobol I. M., Syunyaev R. A., 1983, Astrophysics and Space Physics Reviews, 2, 189
- Poutanen J., & Gierliński M. 2003, MNRAS, 343, 1301
- Remillard R. A., & McClintock J. E., 2006, ARA&A, 44, 49
- Revnivstev M., Gilfanov M., Churazov E., 1999, A&A, 347, L23
- Ross R. R., Fabian A. C., 2005, MNRAS, 358, 211
- Smith D. A., 1998, IAU Circ. 7008
- Sobolewska M. A., Życki P. T., 2006, MNRAS, 370, 405
- Veledina A., Poutanen J., Vurm I., 2013, MNRAS, 430, 3196
- Veledina A., Poutanen J., Ingram A., 2013, in prep.
- Viironen K., & Poutanen J., 2004, A&A, 426, 985
- Yamada S., Makishima K., Done C. et al., 2013, arXiv:1304.1968
- Young A. J., Fabian A. C., Ross R. R., Tanaka Y., 2001, MNRAS, 325, 1045
- Życki P., Done C., Smith D.A., 1999, MNRAS, 309, 561